Electron-phonon interaction effects in semiconductor quantum dots: A nonperturabative approach

M. I. Vasilevskiy*

Centro de Física, Universidade do Minho, 4710-057 Braga, Portugal

E. V. Anda[†]

Departamento de Física, Pontifícia Universidade Católica, Rio de Janeiro-RJ, Brazil

S. S. Makler[‡]

*Instituto de Física, Universidade Federal Fluminense, Niterói, RJ, Brazil and Instituto de Física,
Universidade do Estado do Rio de Janeiro, Rio de Janeiro-RJ, Brazil*

Multiphonon processes in a model quantum dot (QD) containing two electronic states and several optical phonon modes are considered by taking into account both intra- and interlevel terms. The Hamiltonian is exactly diagonalized, including a finite number of multiphonon processes large enough to guarantee that the result can be considered exact in the physically important energy region. The physical properties are studied by calculating the electronic Green's function and the QD dielectric function. When both the intra- and interlevel interactions are included, the calculated spectra allow several previously published experimental results obtained for spherical and self-assembled QD's, such as enhanced two-LO-phonon replica in absorption spectra and up-converted photoluminescence to be explained. An explicit calculation of the spectral line shape due to intralevel interaction with a continuum of acoustic phonons is presented, where the multiphonon processes also are shown to be important. It is pointed out that such an interaction, under certain conditions, can lead to relaxation in the otherwise stationary polaron system.

I. INTRODUCTION

The importance of phonon influence on the properties of semiconductor quantum dot (QD) based systems has been demonstrated in many works reviewed in Refs. 1 and 2. The spatial confinement effect on optical phonons in QD's has been studied both experimentally and theoretically.[3–7] Acoustic phonons have also received some attention in connection with the low-frequency Raman scattering in spherical[8,9] and self-assembled[10,11] QD's, and the homogeneous broadening of the spectral lines.[12–14] Electron-phonon interaction in QD's remains, however, a controversial subject. While calculations performed for II-VI and III-V dots generally agree that the exciton-phonon (e-ph) coupling strength is reduced in nanocrystals compared to the bulk, they disagree regarding the numbers and trends in the scale of the interaction with QD size. (Here electron-hole pairs will be called excitons independently of the importance of the Coulomb interaction.) The calculated values vary substantially depending on the approximations used, but the Huang-Rhys parameter for the lowest exciton state usually does not exceed $S \approx 0.1$–0.2 for II-VI for spherical QD's (Refs. 15 and 16) and is probably an order of magnitude smaller for III-V self-assembled dots.[17]

Turning to the experimental data, the exciton-optical-phonon coupling strength is most frequently obtained using photoluminescence (PL) spectra. Usually in small II-VI QD's there is a large Stokes shift of the excitonic PL band with respect to the absorption,[1,18] which can be explained by strong exciton-phonon coupling [Huang-Rhys parameter of

the order of I (Refs. 19 and 20)]. However, as mentioned above, the calculated values happen to be one or two orders of magnitude smaller. Phonon replicas in the PL spectra caused by the recombination of excitons in QD's were found to disagree with the well-known Franck-Condon progression, both in their spectral positions[20,21] and relative intensities.[20,22,23] Although both the strong Stokes shift and apparently large intensity of the first phonon satellite (relative to the zero phonon line) can be characteristic of the QD size distribution and not of a single dot,[18] these results indicate that the e-ph interaction in QD's must be considered carefully. Further evidence for unexpected effects of the e-ph interaction comes from the optical absorption measurements. LO-phonon related features were observed in absorption spectra of InAs/GaAs QD's and two-LO-phonon[24–27] and even three-LO-phonon[28] replicas were found to be extraordinarily strong compared to the one-LO-phonon satellite. At least some of these works were performed using single QD spectroscopy, so ensemble effects can probably be ruled out in this case. Since no phonon replicas were found in the corresponding emission spectra, there is no way to explain these results in terms of the Franck-Condon progression (with any value of S). The temperature dependence of the homogeneous broadening of the absorption spectra of spherical II-VI QD's studied in Refs. 15 and 29 was found to have a clear contribution from optical phonons. This is unexpected, because the coupling of optical phonons to a single electron or exciton level should lead to the appearance of discrete satellites and not to an overall broadening. Thinking in terms of Fermi's golden rule, the broadening could be a

lifetime effect from an electron (or exciton) transition to another state with emission or absorption of an optical phonon. However, the process should strictly adhere to the conservation of energy in the electron-phonon scattering, i.e., exact resonance between the optical phonon energy and level spacing, which should be rather accidental. This argument justified the theoretical concept of "phonon bottleneck," a very slow carrier relaxation which should be inherent to small QD's.[2] Nevertheless, an efficient phonon-mediated carrier relaxation has been reported in a number of works.[21,28,30] All these experimental results imply that multiphonon processes are important and that the e-ph interaction in QD's must be treated in a nonperturbative way, even for the moderate values of the coupling constants coming out from the calculations.[31] An important ingredient to be included is the nonadiabaticity of this interaction,[2,7,22] leading to a phonon-mediated coupling of different electronic levels, even if they are separated by an energy quite different from the optical phonon energy. This is essential for understanding those experimental results which are in clear disagreement with the single-level-generated Franck-Condon progression.[32]

Polaron effects in QD's have been studied theoretically in several recent papers.[33–37] The model considered in these works included two electronic levels and several Einstein phonon modes. The one-electron spectral function was obtained either applying self-consistent perturbation theory approximations[33,34] or exactly, using a combined analytical and numerical approach.[35] The results calculated using the perturbation theory approaches show shift and broadening of the levels, even for a sufficiently large detuning [defined as $\Delta' = \Delta - \hbar\omega_0$ where $\Delta = (\varepsilon_2 - \varepsilon_1)$, ε_1 and ε_2 are the electron energy levels and $\hbar\omega_0$ is the phonon energy]. However, as pointed out in Refs. 35 and 38, this broadening is an artifact as the exact spectral function should consist of δ functions (if no further effects are involved). Moreover, even if these δ functions are broadened artificially, the self-consistent perturbation theory approximations are not able to reproduce the structure of the spectrum calculated exactly using the approach proposed in Ref. 35. The method of Ref. 35 based on the Gram-Schmidt orthogonalization procedure is, however, limited to the case when all the optical phonons have the same energy. The same restriction was used in Ref. 36 (and, in addition, states with more than two phonons and some virtual transitions were excluded from consideration). In reality, confined optical phonon modes are characterized by different frequencies within the band of the corresponding bulk material. Usually there are a small number of such modes that interact more intensely with electrons or excitons.[4,6,39] The incorporation of this multiplicity seems to be important for comparison of calculated and experimental results. It has been possible in the approach proposed in Ref. 37 (based on the Davydov canonical transformation), which, however, neglects multiphonon processes.

Another important issue is the role of acoustic phonons. Even though some acoustic modes can be confined to the QD and therefore have discrete energies, there should be a continuum of modes within a certain energy range. The interaction with this continuum should smooth out the polaron spectrum (otherwise consisting of δ functions, as noted above). The line shape for a QD is not expected to be a simple Lorentzian; instead, for a discrete electronic level acoustic phonon sidebands are formed.[14,40] Considering that the simultaneous interaction of confined excitons with acoustic and optical phonons can reveal some new effects, to the best of our knowledge, this has not been performed beyond the one-level model.[41]

In this paper, we propose a nonperturbative approach to the calculation of the phonon effects on the electron spectral function, and QD emission and absorption spectra, based on the direct numerical diagonalization of the Hamiltonian matrix including a small number of electronic levels and several optical phonon modes of different energy. Such a straightforward method was employed in Ref. 42 for phonons strongly coupled to an electron on a deep donor center. This approach is developed further here, so as to allow for the incorporation of the interaction with (virtually all) acoustic phonon modes under the condition that the interlevel coupling mediated by solely acoustic phonons can be neglected. We present the calculated results which elucidate the influence of various relevant parameters, such as interlevel spacing, coupling strengths, and temperature, on the optical spectra of a model QD. The paper is organized as follows. In Sec. II, we introduce the Hamiltonian matrix to be diagonalized in order to obtain the polaron states, and define the electron Green's function. In Sec. III, we derive the expression for the imaginary part of the exciton dielectric function and present the absorption and emission spectra calculated for different values of the relevant parameters. Section IV is devoted to the interaction with acoustic phonons and its incorporation in the calculation of the polaron spectra. The calculated results and their comparison with experimental data are discussed in Sec. V.

II. ELECTRON-OPTICAL-PHONON INTERACTION: THE NONPERTURBATIVE SOLUTION

Our model system consists of two electronic levels, both coupled to N phonon modes (of frequencies ω_ν), and is described by the Hamiltonian,

$$H_1 = \sum_{i=1}^{2} \varepsilon_i a_i^\dagger a_i + \sum_{\nu=1}^{N} \hbar\omega_\nu b_\nu^\dagger b_\nu + \sum_{ij}^{2} \sum_{\nu=1}^{N} g_{ij}^\nu a_i^\dagger a_j (b_\nu^\dagger + b_\nu),$$

(1)

where $a_i^\dagger$ and a_i are the fermion creation and annihilation operators of the electrons (or holes) and $b_\nu^\dagger$ and b_ν are the operators for the phonons. The interaction with optical phonons occurs predominantly through the Fröhlich-type mechanism and the Hamiltonian matrix elements between exciton states i and j are given by[4,6]

$$g_{ij}^\nu = e \int \Psi_i^*(\vec{r}_e, \vec{r}_h)[\phi_\nu(\vec{r}_h) - \phi_\nu(\vec{r}_e)]\Psi_j(\vec{r}_e, \vec{r}_h) d\vec{r}_e d\vec{r}_h, \quad (2)$$

where ϕ_ν is the electrostatic potential created by the νth phonon mode and Ψ_i is the exciton wave function of state i. In the following, we shall also use dimensionless interaction constants $\alpha_{ij}^\nu = g_{ij}^\nu/(\hbar\omega_\nu)$ and omit the superscript when only one phonon mode is considered.

If g_{12}^ν were equal to zero, the Hamiltonian (1) would be exactly solvable, as there would be no interference between two electronic levels. The one-level model (known as independent boson model) has an analytical solution.[43] The polaron spectrum, in the case of a single phonon mode, consists of equidistant peaks (separated by the phonon energy $\hbar\omega_0$), which is the origin of the Franck-Condon progression.

The case of $\alpha_{12} \neq 0$, $\alpha_{11} = \alpha_{22} = 0$ for a single phonon mode, in the so-called rotation wave (RW) approximation[44] [which consists in neglecting virtual transitions described by the terms $a_2^\dagger a_1 b_0^\dagger$ and $a_2 a_1^\dagger b_0$ in Eq. (1)], also provides an analytical solution, with the spectrum given by

$$E_{1,2}(m) = (\Delta'/2) \pm \sqrt{(\Delta'^2/4) + (m+1)(g_{12})^2} + (m+1)\hbar\omega_0,$$
(3)

where $m = 0, 1, 2, \ldots$ is the number of phonons in the mixed state. In addition to Eq. (3), there is a state with $E = 0$.

The general case, which is of interest here, can be treated by mapping the many-body problem onto a single-particle problem in a higher dimension Fock space.[45,46] It is natural to consider a basis $|n_1 n_2 \{m_\nu\}\rangle$ where $n_r = 0$, 1 is the number of fermions on level r and m_ν is the number of phonons of mode ν. In principle, the Hamiltonian matrix is infinite, but as it will be shown below, one can truncate the Fock space by allowing a certain maximum number of phonons for each mode to obtain a very accurate solution. Since we are interested in the case when there is a single fermion in the dot, it is only necessary to consider the states $|10\{m_\nu\}\rangle$ and $|01\{m_\nu\}\rangle$. The required matrix elements are

$$H_{ij} = \left[\varepsilon_i \delta_{ij} + \sum_{\nu=1}^N m_\nu \hbar\omega_\nu \right] \prod_\nu \delta_{m'_\nu m_\nu} + \sum_{\nu=1}^N g_{ij}^\nu [\sqrt{m_\nu + 1}\, \delta_{m'_\nu m_\nu + 1}$$
$$+ \sqrt{m_\nu}\, \delta_{m'_\nu m_\nu - 1}] \prod_{\mu \neq \nu} \delta_{m'_\mu m_\mu},$$

where i and j represent the basis vectors $|10\{m_\nu\}\rangle$ ($i=1$) and $|01\{m_\nu\}\rangle$ ($i=2$). The dimension of the matrix is $2m_1 \cdots m_\nu \cdots m_N$. For a small number of modes and a reasonable number of phonons for each mode, it can be easily diagonalized numerically. Given the eigenstates of the Hamiltonian matrix (denoted by $|k\rangle$), we can write down the electron Green's function.[47] In the canonical ensemble,

$$G_{ij}(E) = \frac{1}{Z} \sum_{kk'} (e^{-\beta E_k} + e^{-\beta E_{k'}}) \frac{\langle k|a_i^\dagger|k'\rangle \langle k'|a_j|k\rangle}{E - (E_k - E_{k'}) - i\eta},$$
(4)

where $\beta = 1/(k_B T)$ and $Z = \text{Tr} \exp(-\beta H)$. Although η in Eq. (4) should be infinitesimal, for computational purposes we suppose it to be a small quantity. Equation (4) can be rewritten as

$$G_{ij}(E) = \frac{1}{Z} \sum_{kk'} e^{-\beta E_k} \left\{ \frac{\langle k|a_i^\dagger|k'\rangle \langle k'|a_j|k\rangle}{E - (E_k - E_{k'}) - i\eta} \right.$$
$$\left. + \frac{\langle k|a_j|k'\rangle \langle k'|a_i^\dagger|k\rangle}{E + (E_k - E_{k'}) - i\eta} \right\}.$$
(5)

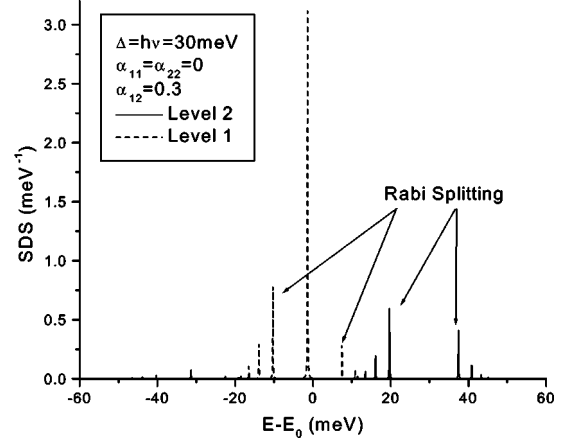In the first term inside the curly brackets, the state $|k\rangle$ has one

FIG. 1. Calculated partial spectral densities of states corresponding to two electronic levels separated by $\Delta = 30$ meV interacting with one optical phonon mode with $\hbar\omega_0 = 30$ meV ($\Delta' = 0$). Only nondiagonal coupling was included ($\alpha_{12} = 0.3$). $T = 300$ K. Note the Rabi splitting in the polaron states and their shift to the lower energies.

electron and the intermediate state $|k'\rangle$ has only phonons. The opposite occurs in the second term. Admitting that it uses infinite energy to create a two-electron state, $|11\{m_\nu\}\rangle$ cannot occur as the intermediate state in Eq. (5). Therefore, we can write for the diagonal elements of the Green's function

$$G_{ii}(E) = \frac{1}{Z} \sum_{kk'} \left[e^{-\beta E_k} + \exp\left(-\beta \sum_\nu m_\nu \hbar\omega_\nu\right) \right]$$
$$\times \frac{|C_i^k(\{m_\nu\})|^2}{E - \left(E_k - \sum_{\nu=1}^N m_\nu \hbar\omega_\nu\right) - i\eta},$$
(6)

where $C_i^k(\{m_\nu\})$ are the eigenvectors expressed in terms of the basis vectors. From Eq. (6), the fermion spectral density of states (SDS) is immediately obtained,

$$\rho(E) = \frac{1}{\pi} \text{Im} \sum_{i=1,2} G_{ii}(E) \equiv \sum_{i=1,2} \rho_i,$$

where ρ_i is the partial SDS corresponding to the ith bare electronic level.

The maximum number of phonons necessary to correctly reproduce several lowest-energy eigenvalues (which are important for temperatures used in the experiments) depends on the coupling strengths but is not large. Just taking 10 as the maximum number of phonons allowed in the system, we obtained the eigenvalues coinciding with the analytical results of Ref. 43 (for $\alpha_{12} = 0$, $\alpha_{11} = \alpha_{22} = 0.2 - 0.3$) and formula (3) (for $\alpha_{12} = 0.2 - 0.3$, $\alpha_{11} = \alpha_{22} = 0$ and using the RW approximation) to within 10^{-3} meV. For example, the SDS spectra calculated for the latter case (but beyond the RW approximation) are shown in Fig. 1.

III. EMISSION AND ABSORPTION SPECTRA

One can calculate the optical absorption and emission spectra using the Kubo formula for the frequency-dependent dielectric function.[43] The imaginary part of the dielectric function, which describes the absorption and emission properties, is related to the real part of the frequency-dependent conductivity by the relation

$$\text{Im } \varepsilon(\omega) = \frac{4\pi}{\omega} \text{Re } \sigma(\omega). \tag{7}$$

According to the Kubo formula,

$$\text{Re } \sigma(\omega) = \frac{e^2}{m_0 V} \frac{1}{2\omega} \int_{-\infty}^{\infty} dt e^{i\omega t} \langle j^\dagger(t) j(0) \rangle. \tag{8}$$

We are interested in describing the transitions from an electron state (labeled 0) in the valence band (which we assume is not phonon coupled) to the states ($i=1,2$) in the conduction band, and *vice versa*. Thus, the current operator is defined as

$$j = \sum_{i=1}^{2} p_{0i}(a_i^\dagger a_0 - a_0^\dagger a_i), \tag{9}$$

where p_{0i} is the momentum matrix element between the corresponding bare states. The current-current correlation function is

$$\langle j^\dagger(t) j(0) \rangle = \sum_{i,i'=1,2} p_{0i}^* p_{0i'} \langle [a_0^\dagger(t) a_i(t) - a_i^\dagger(t) a_0(t)]$$
$$\times [a_0^\dagger a_{i'} - a_{i'}^\dagger a_0] \rangle. \tag{10}$$

This expression can be developed into four expectation values. However, there are only two terms which contribute to the sum in Eq. (10). This occurs because $a_i|k\rangle$ vanishes if $|k\rangle$, an eigenstate of the Hamiltonian (1), is a state with zero electrons. The nonzero terms are

$$\langle a_0^\dagger(t) a_i(t) a_{i'}^\dagger a_0 \rangle = \frac{1}{Z} \sum_k e^{-\beta E_k} e^{iE_k t} \langle k | a_0^\dagger a_i e^{-iHt} a_{i'}^\dagger a_0 | k \rangle$$

and

$$\langle a_i^\dagger(t) a_0(t) a_0^\dagger a_{i'} \rangle = \frac{1}{Z} \sum_k e^{-\beta E_k} e^{iE_k t} \langle k | a_i^\dagger a_0 e^{-iHt} a_0^\dagger a_{i'} | k \rangle,$$

where $a_i \equiv a_i(0)$. These terms can be evaluated using the identity $1 = \Sigma_{k'} |k'\rangle\langle k'|$ by inserting unity between the a operators. The result is

$$\langle j^\dagger(t) j(0) \rangle = \frac{1}{Z} \sum_{k,\{m_\nu\}} \sum_{i,i'} p_{0i}^* p_{0i'} e^{-\beta E_k} e^{i(E_k - E_0)t}$$
$$\times [C_{i'}^{k*}(\{m_\nu\}) C_i^k(\{m_\nu\}) - C_i^{k*}(\{m_\nu\}) C_{i'}^k(\{m_\nu\})]. \tag{11}$$

Using Eq. (11), performing the Fourier transformation in Eq.

(8) and substituting in Eq. (7), we obtain the following expression for the imaginary part of the dielectric function:

$$\text{Im } \epsilon(\omega) = \left(\frac{2\pi e}{m_0 \omega}\right)^2 \frac{1}{VZ'} \sum_{i,i'=1,2} \Bigg\{ p_{0i}^* p_{0i'}$$
$$\times \sum_{k,\{m_\nu\}} \exp\left(-\beta \sum_\nu m_\nu \hbar \omega_\nu\right) C_i^{k*}(\{m_\nu\}) C_{i'}^k(\{m_\nu\})$$
$$\times \Bigg[\delta\left(\omega - \left(E_k - \sum_\nu m_\nu \hbar \omega_\nu\right)\right) + \exp\Big(-\beta\Big(E_k$$
$$- \sum_\nu m_\nu \hbar \omega_\nu\Big)\Big) \delta\left(\omega + \left(E_k - \sum_\nu m_\nu \hbar \omega_\nu\right)\right) \Bigg] \Bigg\},$$
$$\tag{12}$$

where $Z' = \Sigma_{\{m_\nu\}} \exp[-\beta \Sigma_\nu m_\nu \hbar \omega_\nu]$. The terms in the second line of Eq. (12) correspond to the absorption and emission, respectively, of a photon of frequency ω. Some absorption and emission spectra, calculated for a hypothetical QD, are presented in Figs. 2–5 (the parameters are indicated on the figures). These demonstrate the effects of the diagonal and off-diagonal coupling strength, interlevel spacing, and temperature on the optical properties of the dot. Here we considered the lower exciton level optically active and the upper one inactive ($p_{02}=0$). Such a situation occurs in spherical II-VI (e.g., CdSe) QD's ($1s_e 1S_{3/2}$ and $1s_e 1P_{3/2}$ states, respectively).[48]

IV. INTERACTION WITH ACOUSTIC PHONONS

Interaction with confined longitudinal acoustic phonons, although mediated by a different mechanism (namely, a deformation potential instead of the Fröhlich potential), can be considered in the same way as for optical phonons and should result in series of closely spaced but still isolated spectral peaks. However, for any kind of QD's embedded in a matrix, there must be a spectral region where acoustic phonons are essentially delocalized and their energy varies in a continuous way. If the velocity of sound in the QD and matrix material is not very different, the density of acoustic phonon states should be similar to that of the bulk crystals. These states can be characterized by a wave vector **q**. This is the case of self-assembled QD's[11] and can be a reasonable approximation for a certain fraction of acoustic phonons in a spherical QD embedded in a dielectric matrix. In this section we shall consider the interaction of an electron localized in the dot with acoustic phonons which are completely delocalized (see Appendix for details). The interaction, which occurs only inside the QD, is weak for each phonon mode (since it contains a factor V_{QD}/V, V is the volume of the whole system). However, since the number of modes is virtually infinite, perturbation theory may fail and we shall avoid using it. For this, we will have to neglect coupling between different electronic levels through acoustic phonons and consider a single electronic level coupled to an arbitrary number of phonon modes. This approximation corresponds to the independent boson model,[43] which is normally considered for optical phonons (see Sec. III). Recently,[14,40] it was applied to acoustic phonons in a QD. Based on the exact
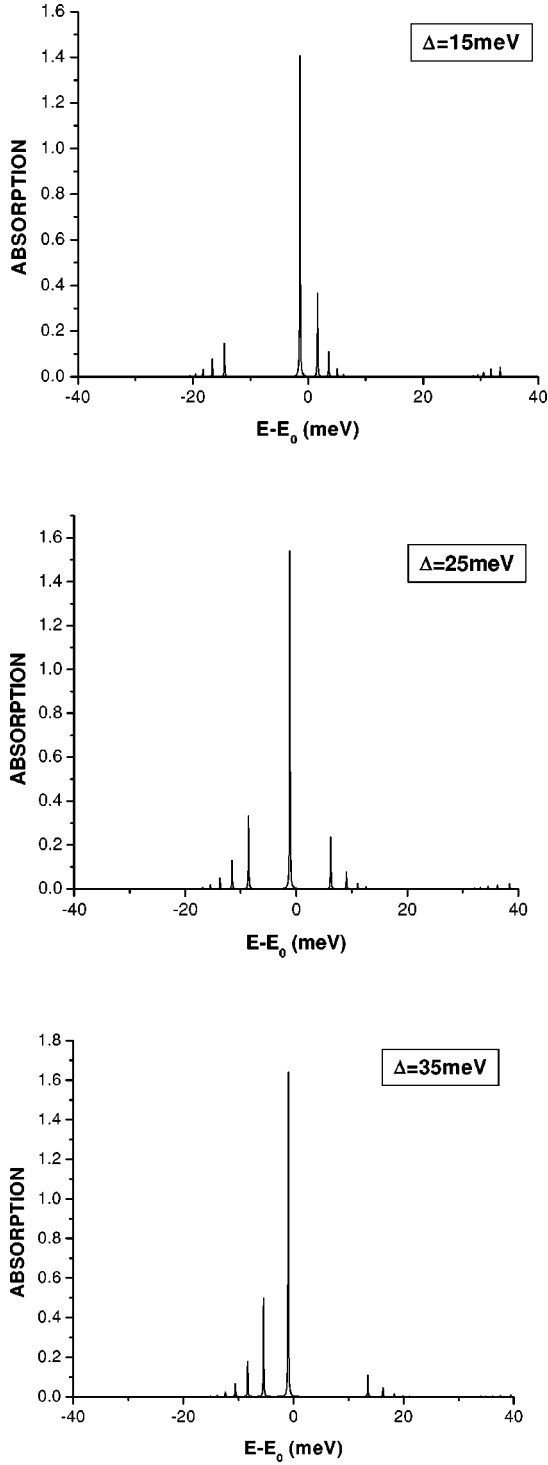
$$H_2 = a^\dagger a \left(\varepsilon_0 + \sum_{\mathbf{q}} g_{\mathbf{q}} (b_{\mathbf{q}}^\dagger + b_{\mathbf{q}}) \right) + \sum_{\mathbf{q}} \hbar \omega_{\mathbf{q}} b_{\mathbf{q}}^\dagger b_{\mathbf{q}}. \quad (13)$$

It can be diagonalized by transformation to new bosonic operators[43]

$$B_{\mathbf{q}} = b_{\mathbf{q}} + \alpha_{\mathbf{q}} a^\dagger a, \quad (14)$$

where $\alpha_{\mathbf{q}} = (g_{\mathbf{q}}/\hbar\omega_{\mathbf{q}})$. The energy spectrum is given by

$$E(\{N_{\mathbf{q}}\}) = \varepsilon_0' + \sum_{\mathbf{q}} \hbar\omega_{\mathbf{q}} N_{\mathbf{q}} \quad (15)$$

with $\varepsilon_0' = \varepsilon_0 - \sum_{\mathbf{q}} \alpha_{\mathbf{q}}^2 \hbar\omega_{\mathbf{q}}$. Eigenstates of the Hamiltonian (13) can be expressed in terms of the pure phonon states,

$$|N_{\mathbf{q}}\rangle' = \sum_{m_{\mathbf{q}}} C_N^m |m_{\mathbf{q}}\rangle. \quad (16)$$

Acting with the operator $B_{\mathbf{q}}^\dagger B_{\mathbf{q}}$ on the wave function (16) we can find recurrent relations for the coefficients C_N^m:

$$N = (m + \alpha_{\mathbf{q}}^2)(C_N^m)^2 + \alpha_{\mathbf{q}}[\sqrt{m+1}\, C_N^{m+1} C_N^m + \sqrt{m}\, C_N^{m-1} C_N^m]. \quad (17)$$

In the linear approximation (with respect to the interaction with a single phonon mode $\mathbf{q}$), we obtain from Eqs. (16) and (17):

$$|N_{\mathbf{q}}\rangle' = p_{N_{\mathbf{q}}} [\sqrt{N_{\mathbf{q}}}\, \alpha_{\mathbf{q}} |N_{\mathbf{q}} - 1\rangle + |N_{\mathbf{q}}\rangle + \sqrt{N_{\mathbf{q}}+1}\, \alpha_{\mathbf{q}} |N_{\mathbf{q}} + 1\rangle], \quad (18)$$

where

$$p_{N_{\mathbf{q}}} = \frac{1}{\sqrt{1 + (2N_{\mathbf{q}} + 1)\alpha_{\mathbf{q}}^2}}.$$

The one-electron Green's function corresponding to the Hamiltonian (13) can now be calculated using Eq. (4),

$$G(E)$$
$$= \left\langle \sum_{\{m_{\mathbf{q}}\}} \frac{\prod_{\mathbf{q}} \{\delta_{m_{\mathbf{q}}, N_{\mathbf{q}}} + \alpha_{\mathbf{q}}^2 [N_{\mathbf{q}} \delta_{m_{\mathbf{q}}, N_{\mathbf{q}}-1} + (N_{\mathbf{q}}+1)\delta_{m_{\mathbf{q}}, N_{\mathbf{q}}+1}]\}}{E - \varepsilon_0' - \sum_{\mathbf{q}} \hbar\omega_{\mathbf{q}}(N_{\mathbf{q}} - m_{\mathbf{q}}) - i\eta} \right.$$
$$\left. \times \exp\left[-\sum_{\mathbf{q}} (2N_{\mathbf{q}} + 1)\alpha_{\mathbf{q}}^2\right] \right\rangle, \quad (19)$$

where the angular brackets stand for the thermodynamical average and the exponential factor arises from the product $\prod_{\mathbf{q}} p_{N_{\mathbf{q}}}$. Taking into account only one-phonon processes, the thermodynamical average approximately replaces $N_{\mathbf{q}}$'s with the corresponding Bose factors $\bar{N}_{\mathbf{q}} = [\exp(\beta\hbar\omega_{\mathbf{q}}) - 1]^{-1}$ and the Green's function can be written as
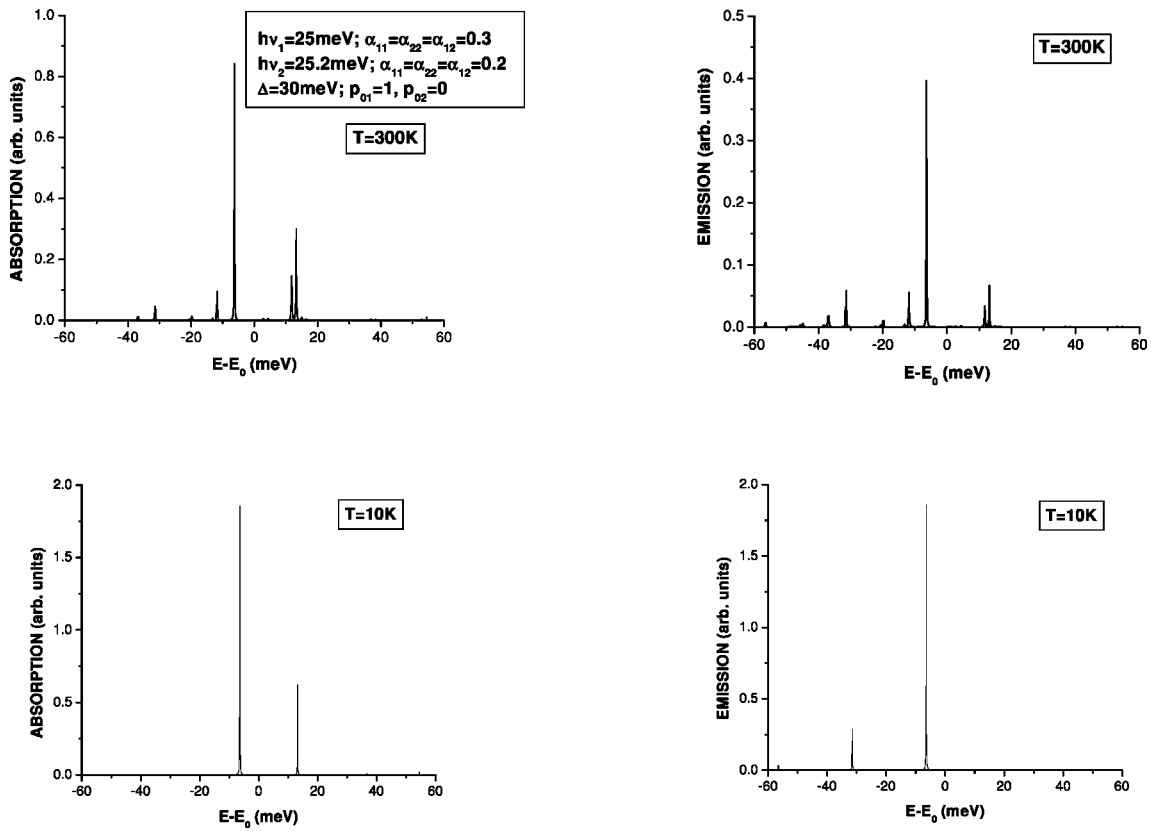

FIG. 2. Calculated room temperature absorption spectra for different values of level spacing as indicated. All the other parameters are the same as for Fig. 1.

solution of this model, we shall propose a different procedure which will lead us directly to the self-energy function of the electron or exciton. Later, this self-energy will be reinterpreted for the optical-phonon polaron.

The Hamiltonian of a system consisting of one electronic level and a continuum of acoustic phonon modes is

FIG. 3. Absorption (left) and emission (right) spectra for a system of two exciton levels separated by $\Delta = 30$ meV calculated for different temperatures. The excitons interact with two optical phonon modes of the energies $\hbar\omega_1 = 25$ meV and $\hbar\omega_2 = 25.2$ meV. The electron-phonon coupling constants are indicated in the figure. The origin of the energy axis is chosen at the energy of the lowest exciton state (E_0).
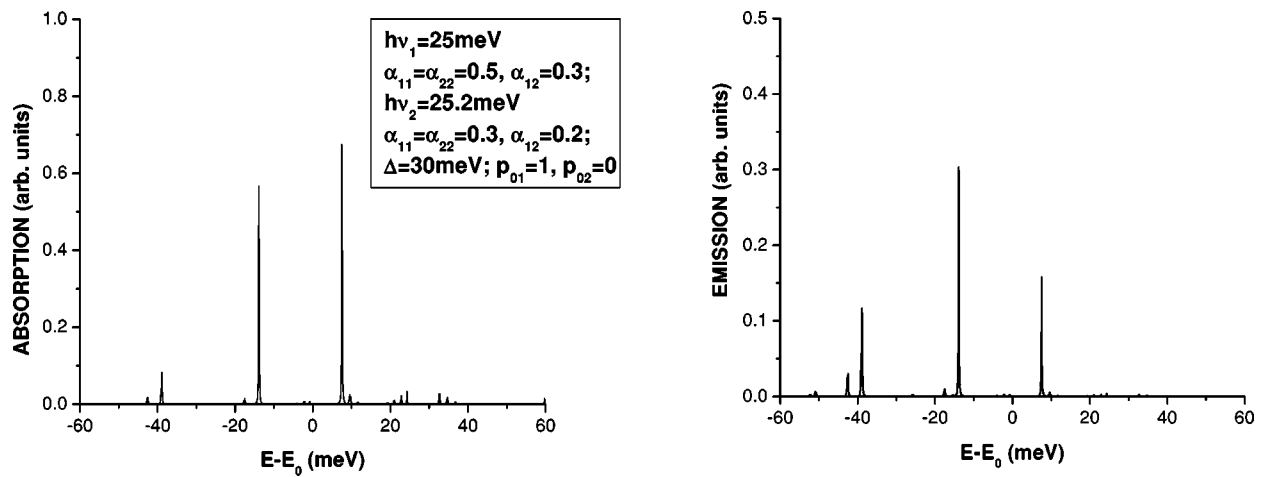

FIG. 4. Absorption (left) and emission (right) spectra calculated for different (compared to Fig. 3) values of the diagonal coupling constants.
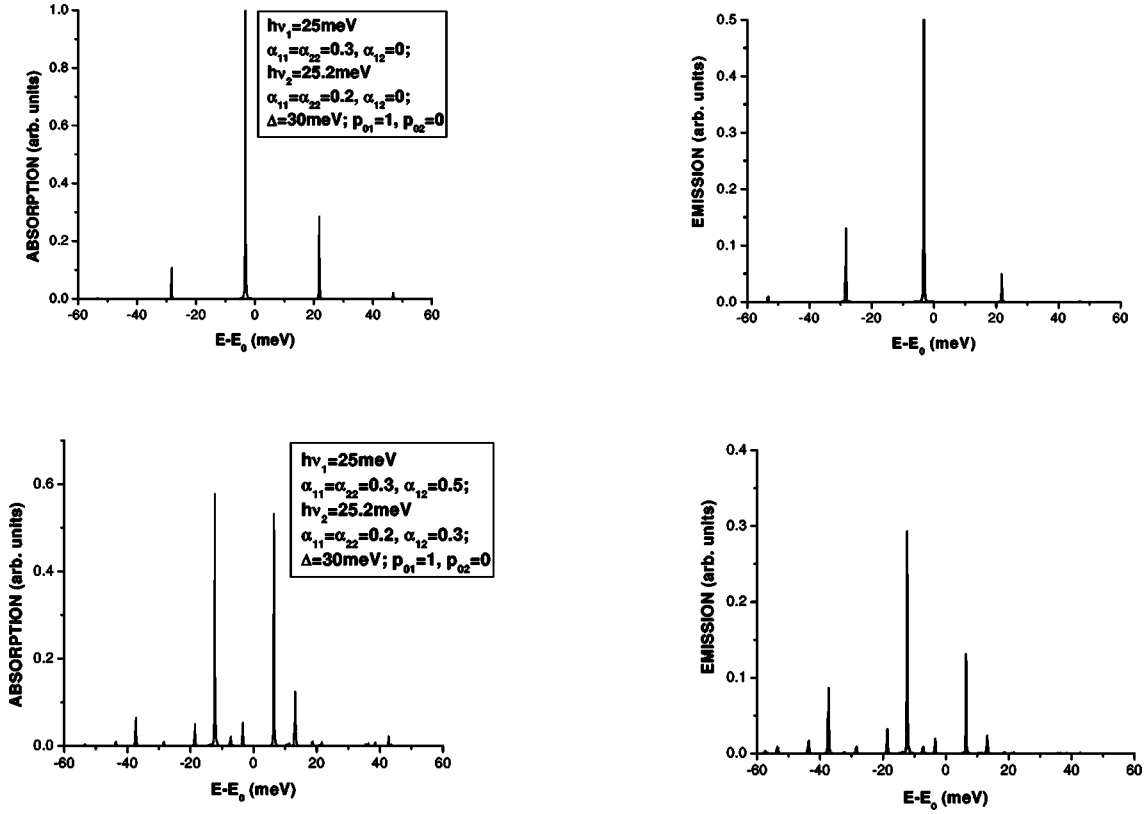
FIG. 5. Absorption (left) and emission (right) spectra calculated for different values of the nondiagonal coupling constant (see the explanation to Fig. 3).

$$G(E) = \left\{ \frac{1}{E - \varepsilon_0' - i\eta} + \sum_{\mathbf{q}} \left[\frac{\alpha_{\mathbf{q}}^2 \bar{N}_{\mathbf{q}}}{E - \varepsilon_0' - \hbar\omega_{\mathbf{q}} - i\eta} \right. \right.$$
$$\left. \left. + \frac{\alpha_{\mathbf{q}}^2 (\bar{N}_{\mathbf{q}} + 1)}{E - \varepsilon_0' + \hbar\omega_{\mathbf{q}} - i\eta} \right] \right\} \left[1 + \sum_{\mathbf{q}} (2\bar{N}_{\mathbf{q}} + 1)\alpha_{\mathbf{q}}^2 \right]^{-1}. \tag{20}$$

However, Eq. (20) can only be used for a quite weak interaction or at very low temperatures. Although the interaction is weak for each phonon mode (all $\alpha_{\mathbf{q}}$ are small), the number of modes is large and the effective electron-phonon interaction is strong. A typical number of phonons interacting with the electron can be estimated as $Q = (2\bar{N}_{\mathbf{q}} + 1)\alpha_{\mathbf{q}}^2$ and for the model presented in Appendix, $Q \gg 1$ for usual experimental temperatures. Under these conditions, it is necessary to use the general equation (19).

The evaluation of the Green's function from Eq. (19) can be made using a Monte Carlo procedure. Instead of summing over all 3^N configurations $\{m_{\mathbf{q}}\}$ (N is the number of acoustic phonon modes), one can generate some N_{MC} most probable configurations with $m_{\mathbf{q}} = (N_{\mathbf{q}} - 1)$, $N_{\mathbf{q}}$, $(N_{\mathbf{q}} + 1)$, occurring with the probabilities $\alpha_{\mathbf{q}}^2 \bar{N}_{\mathbf{q}} p_{\bar{N}_{\mathbf{q}}}^2$, $p_{\bar{N}_{\mathbf{q}}}^2$, and $\alpha_{\mathbf{q}}^2 (\bar{N}_{\mathbf{q}} + 1) p_{\bar{N}_{\mathbf{q}}}^2$, respectively. Averaging over a sufficiently large N_{MC} of such configurations, $G(E)$ is obtained including all the many-phonon processes.

Let us define the electron self-energy taking into account the interaction with acoustic phonons,

$$\Sigma(E) = E - G^{-1}(E). \tag{21}$$

In the one-phonon approximation, the explicit expression for the self-energy is

$$\Sigma(E) = \varepsilon_0' - (E - \varepsilon_0') \sum_{\mathbf{q}} \alpha_{\mathbf{q}}^2 (2\bar{N}_{\mathbf{q}} + 1)$$
$$+ (E - \varepsilon_0')^2 \sum_{\mathbf{q}} \left[\frac{\alpha_{\mathbf{q}}^2 \bar{N}_{\mathbf{q}}}{E - \varepsilon_0' - \hbar\omega_{\mathbf{q}} - i\eta} \right.$$
$$\left. + \frac{\alpha_{\mathbf{q}}^2 (\bar{N}_{\mathbf{q}} + 1)}{E - \varepsilon_0' + \hbar\omega_{\mathbf{q}} - i\eta} \right]. \tag{22}$$

The spectral dependence of the self-energy corresponding to the Green's function [Eq. (20)], obtained using the Monte Carlo procedure, is presented in Figs. 6 and 7. For comparison, we have also calculated the self-energy using Eq. (22). The interaction constants $\alpha_{\mathbf{q}}$, derived in the Appendix, were used in these calculations and the material parameters were those of CdSe, except for the deformation potential constant a_c, which is about 2 times smaller than the bulk value of the relative volume deformation potential between the valence and conduction bands.[49] Such a choice is justified by the fact that only a fraction of acoustic phonons can be described by a propagating wave assumed in the Appendix.

Assuming that the broadening of the electronic levels produced by the interaction with acoustic phonons is small compared to the electronic level spacing, it is possible to include
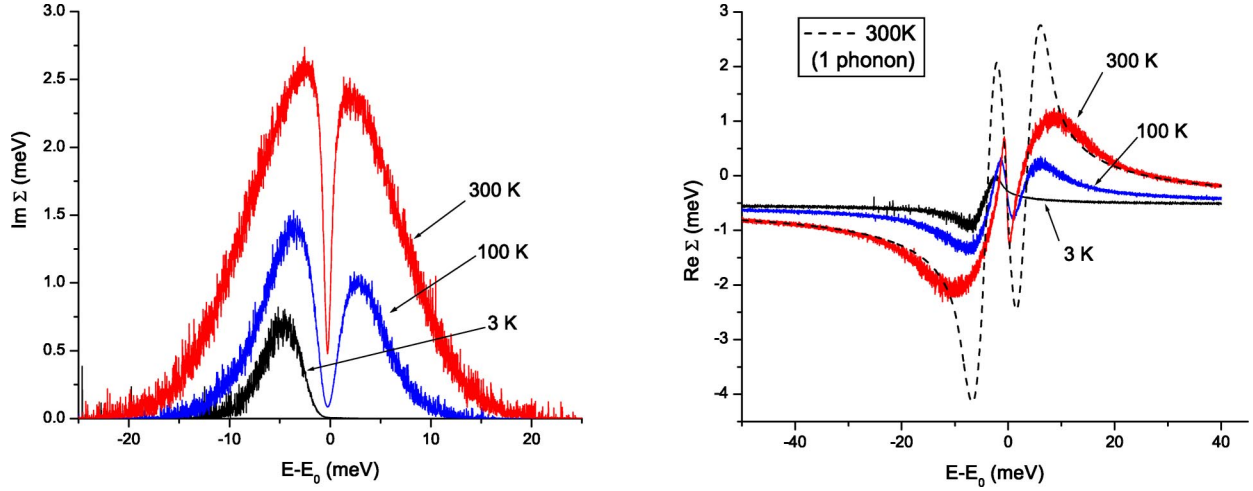
FIG. 6. Imaginary (left) and real (right) parts of the self-energy for a single electronic level interacting with acoustic phonons, calculated for different temperatures using the Monte Carlo technique explained in the text. The dashed curve was plotted using the one-electron approximation [Eq. (22)]. The coupling constants were calculated as explained in the Appendix. The necessary material parameters were taken as follows: $\rho_0 = 5.8 \text{ g/cm}^3$, $c_l = 3.8 \text{ km/s}$ and $a_c = 3.5 \text{ eV}$. The QD radius $R = 2$ nm.

this interaction in our scheme to consider the polaronic states proposed in the previous sections. Let us consider now the full Hamiltonian, which includes the interactions with both optical and acoustic phonons,

$$H_3 = \sum_{i=1}^{2} \left(\varepsilon_i + \sum_{\mathbf{q}} g_{\mathbf{q}}^{(i)} (b_{\mathbf{q}}^{\dagger} + b_{\mathbf{q}}) \right) a_i^{\dagger} a_i + \sum_{ij}^{2} \sum_{\nu=1}^{N} g_{ij}^{\nu} a_i^{\dagger} a_j (b_{\nu}^{\dagger} + b_{\nu})$$

$$+ \sum_{\mathbf{q}} \hbar \omega_{\mathbf{q}} b_{\mathbf{q}}^{\dagger} b_{\mathbf{q}} + \sum_{\nu=1}^{N} \hbar \omega_{\nu} b_{\nu}^{\dagger} b_{\nu}, \quad (23)$$

where $g_{\mathbf{q}}^{(i)}$ denotes the acoustic phonon coupling constant for electronic level i. The Hamiltonian (23) can be rewritten in terms of the polaron states $|k\rangle$ by introducing the corresponding (fermionic) annihilation and creation operators $A_k^{\dagger}, A_k$. The electron–LO-phonon Hamiltonian (1) is then reduced to

$$H_1 = \sum_k E_k A_k^{\dagger} A_k.$$

Using the expansion of the bare electronic states in terms of the polaron ones,

$$|i\rangle = \sum_k \sum_{\{m_\nu\}} [C_i^k(\{m_\nu\})]^* |k\rangle,$$

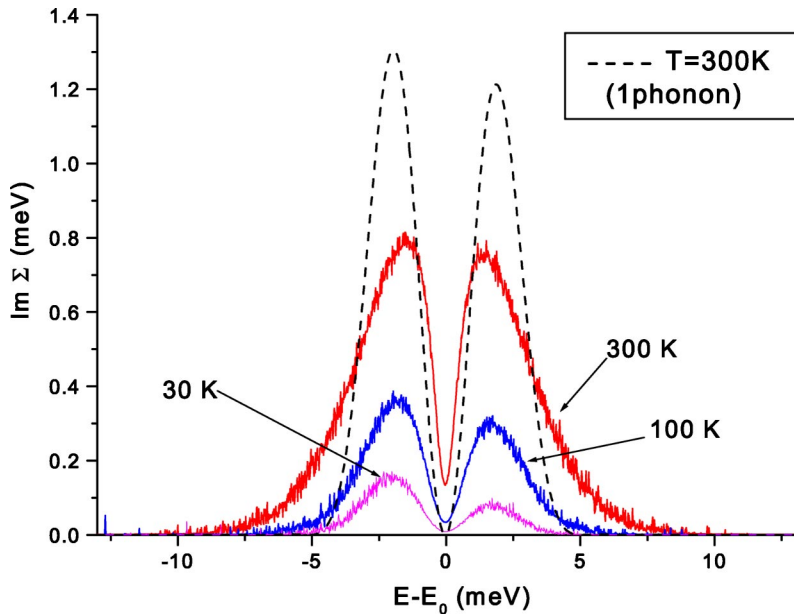the term in Eq. (23) representing the interaction with acoustic phonons can be written as

FIG. 7. Imaginary part of the self-energy calculated for a $R = 4$ nm QD as explained in Fig. 6. The dashed curve was plotted using one-electron approximation [Eq. (22)].

$$\sum_{i=1,2}\sum_{\mathbf{q}} g_{\mathbf{q}}^{(i)}(b_{\mathbf{q}}^{\dagger}+b_{\mathbf{q}})\sum_{k,k'}\sum_{\{m_\nu\}}[C_i^k(\{m_\nu\})]^* C_i^{k'}(\{m_\nu\})A_k^{\dagger}A_{k'}$$

$$=\sum_{\mathbf{q}} g_{\mathbf{q}}(b_{\mathbf{q}}^{\dagger}+b_{\mathbf{q}})\sum_k A_k^{\dagger}A_k + \sum_{\mathbf{q}}\Delta g_{\mathbf{q}}(b_{\mathbf{q}}^{\dagger}+b_{\mathbf{q}})\sum_{k,k'} t_{k,k'}A_k^{\dagger}A_{k'},$$

$$(24)$$

where $g_{\mathbf{q}}=(g_{\mathbf{q}}^{(1)}+g_{\mathbf{q}}^{(2)})/2$, $\Delta g_{\mathbf{q}}=(g_{\mathbf{q}}^{(2)}-g_{\mathbf{q}}^{(1)})$, and

$$t_{k,k'}=\sum_{\{m_\nu\}}\{[C_1^k(\{m_\nu\})]^* C_1^{k'}(\{m_\nu\})-[C_2^k(\{m_\nu\})]^* C_2^{k'}(\{m_\nu\})\}.$$

Neglecting the last term in Eq. (24), that is assuming that the coupling to acoustic phonons is approximately the same for both electronic levels, we arrive at the Hamiltonian

$$H_3=\sum_k A_k^{\dagger}A_k(E_k+\sum_{\mathbf{q}} g_{\mathbf{q}}(b_{\mathbf{q}}^{\dagger}+b_{\mathbf{q}}))+\sum_{\mathbf{q}}\hbar\omega_{\mathbf{q}} b_{\mathbf{q}}^{\dagger}b_{\mathbf{q}}. \quad (25)$$

This can be diagonalized exactly in the same way as Eq. (13). The poles of the electron Green's function (6) (as well as the absorption and emission peaks) are shifted according to the substitution $E_k \to E_k'$,

$$E_k'=E_k-\sum_{\mathbf{q}}\alpha_{\mathbf{q}}^2\hbar\omega_{\mathbf{q}}+\langle\sum_{\mathbf{q}}\hbar\omega_{\mathbf{q}}(N_{\mathbf{q}}-m_{\mathbf{q}})\rangle,$$

where, as before, $(N_{\mathbf{q}}-m_{\mathbf{q}})$ can be considered a random variable taking the values 1, 0, and -1 with the probabilities $\alpha_{\mathbf{q}}^2\bar{N}_{\mathbf{q}} p_{\bar{N}_{\mathbf{q}}}^2$, $p_{\bar{N}_{\mathbf{q}}}^2$, and $\alpha_{\mathbf{q}}^2(\bar{N}_{\mathbf{q}}+1)p_{\bar{N}_{\mathbf{q}}}^2$, respectively. This results in a similar broadening and a downward shift of all the polaron states contributing to the spectral density of states, absorption, and emission, just as in the one-level independent boson model.[41] It is equivalent to ascribing a spectral variable-dependent self-energy, $\Sigma(E-E_p)$ [given by Eq. (21) or (22)], to each pole of Eq. (6). As before, we can reinterpret this result for an exciton-polaron, under the condition that we have no more than one exciton per QD. Examples of spectra showing this effect are presented in Fig. 8. The nondiagonal term with $t_{k,k'}$ leads to an acoustic-phonon-mediated mixing of the polaron states, which will be considered in a future work.

V. DISCUSSION

Let us start the discussion by emphasizing that only in the hypothetical case where the phonon-mediated coupling of the lowest energy exciton state to all other states can be neglected (for example, in the limit of extremely strong confinement, such that $\Delta \gg \hbar\omega_0$, or if α_{12} is small because of the symmetry of the corresponding wave functions), can one expect to observe Franck-Condon progressions in the emission and absorption spectra associated with this state.[41] This is the only case when the Huang-Rhys parameter describes the spectra in the entirety. It is obvious from Eq. (2) that the *diagonal* coupling is proportional to the (integrated) difference between the electron and hole charge densities, which is nonzero mainly due to the fact that the conduction and valence bands in II-VI and III-V materials have different symmetries. Even if some further effects (for example, a presence of defects or strain) contribute to the separation of the
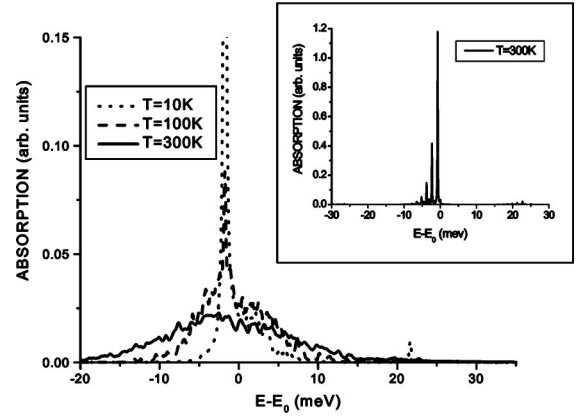

FIG. 8. Absorption spectra calculated for an $R=2$ nm CdSe QD including both optical and acoustic phonons for three different temperatures. Two optical phonon modes of the energies $\hbar\omega_1=25$ meV and $\hbar\omega_2=25.8$ meV and dimensionless interaction constants (divided by the corresponding phonon energies) $\alpha_{11}^1=-0.015$, $\alpha_{22}^2=0.027$, $\alpha_{12}^1=0.295$; $\alpha_{11}^2=0.063$, $\alpha_{22}^2=0.053$, $\alpha_{12}^2=0.095$ calculated in Ref. 39 were used. The acoustic phonon parameters were taken as for Fig. 6. The level spacing of $\Delta=80$ meV was assumed. The inset shows the $T=300\ K$ spectrum without the acoustic phonon contribution (at $T=10\ K$ only the main peak is seen).

electron and hole clouds in space,[17] one can hardly expect an order of magnitude increase in this parameter, compared to the calculated values cited in the Introduction. This means that the intensity of the LO-phonon sidebands must be rather small and monotonically decreasing with the increase of the number of phonons.

However, in most cases the phonon-mediated interlevel coupling, at least between the subsequent exciton states, should be important. The off-diagonal interaction constant is likely to exceed the diagonal ones. For instance, if the two exciton levels are different by the participating hole state (e.g., $1s_e1S_{3/2}$ and $1s_e1P_{3/2}$ states in a spherical II-VI QD), it is easy to see from Eq. (2) that (neglecting the Coulomb interaction between the electron and hole)

$$g_{12}^{\nu}=e\int\Psi_{1h}^*(\vec{r}_h)\phi_\nu(\vec{r}_h)\Psi_{2h}(\vec{r}_h)d\vec{r}_h, \quad (26)$$

that is, there is no compensation effect for this interaction. The spectra calculated assuming only the off-diagonal interaction (Figs. 1 and 2) show characteristic features known as Rabi splitting, which is already present in the RW approximation [see Eq. (3)] and has been observed experimentally.[31] Contrary to the RW approximation, the exact results also show a downwards shift of the spectral lines (see Fig. 1). (In the RW approximation, the most intense peak should be situated exactly at $E-E_0=0$.) It has been noticed in Ref. 32 that the nonadiabaticity results in a shift of the zero-phonon line in the absorption spectrum towards lower energies. Here we have shown that this effect is due to the virtual transitions neglected in the RW approximation. Even if the upper level is dipole forbidden, the phonon-assisted coupling to the optically active level makes it possible the optical transition to

the former.[32] The presence of the optically inactive level manifests itself by the manifolds seen in the spectra of Fig. 2. Note that the off-diagonal coupling is not resonant as one might expect thinking in terms of the Fermi's golden rule. The manifold produced by the coupling persists even for quite a large detuning $\Delta' > \hbar\omega_0$. Curiously, it is reminiscent of sidebands which might appear due to interaction with confined acoustic phonons.

When both diagonal and off-diagonal interactions are present, the effect is not just a sum of each of them, but also some additional spectral features appear (see Figs. 3–5 showing the effect of different parameters). This multiplicity of allowed optical transitions is characteristic of the strong e-ph coupling regime.[36] The stronger the interactions are, the richer the structure of the spectra. It should also be noted that the symmetry between the absorption and emission spectra, which is characteristic of the one-level independent boson model (see the upper panel of Fig. 5), disappears when the off-diagonal interaction is included. This also holds at low temperatures where a small number of spectral features are seen (Fig. 3, lower panel). Those below E_0 in the emission spectrum are due to the diagonal coupling to the lowest energy exciton state. The one seen in the absorption originates from interlevel coupling.

Let us turn to the acoustic phonons. The explicit calculation leads to a self-energy that depends on the spectral variable in a sophisticated way. Accordingly, the line shape is quite different from the simple Lorentzian.[14,40] The noise seen in the calculated spectra of the self-energy (Figs. 6 and 7) is due to the Monte Carlo procedure used, when each configuration $\{m_\mathbf{q}\}$ of phonons produces a δ function and the number of Monte Carlo runs is finite ($N_{MC} = 20\,000$ for Figs. 6 and 7). The imaginary part of the self-energy vanishes at ε_0', so, the zero-phonon line (ZPL) at low temperatures remains a sharp δ-like resonance situated between two asymmetric phonon sidebands, in accordance with experiment[12,13] and previous theoretical studies.[14,40] Only for high temperatures does the SDS generated by a single electronic level take a bell-like shape similar to the Lorentzian. The calculated results also confirm the statement concerning the importance of the multiphonon processes which increase in smaller QD's (Fig. 6). Turning to the exciton-polaron spectrum (Fig. 8), the acoustic phonon-related broadening smears the discrete structure associated with optical phonons. The multiplicity of the confined optical phonon modes also helps this. Below, we shall explain some previously published experimental findings, which were not clearly understood before, in terms of our calculated results.

A. "Strange" phonon replicas

Experimental evidence for spectral features whose distance from ZPL is smaller than the LO-phonon energy was found in several works.[20,21,24,50] Thinking in terms of the Franck-Condon progression, such peaks were attributed to additional (interface or disorder-activated acoustic) phonon modes, for some reason strongly coupled to the exciton.[50] As can be seen from Figs. 3–5, in the presence of interlevel coupling, there are many spectral features that are not separated from the ZPL (the most intense peak in all spectra) by (a multiple of) the optical phonon energy. Some of them persist at low temperatures. Such "strange" replicas can be generated by a *single* phonon mode (long-wavelength LO phonon, neglecting its confinement) and their spectral positions are determined by the e-ph coupling constants. Thus, there is no need to invoke extra modes (for which their strong coupling to the exciton it would be hard to justify) in order to explain these spectral features. The phonon-mediated interlevel coupling provides a simpler and more plausible explanation.

B. Anomalously strong two-LO-phonon satellite

As mentioned in the Introduction, several groups have observed apparently phonon-related features in the absorption (but not in the emission) spectra of resonantly excited self-assembled QD's.[24–28] Given the relative weakness of the exciton-phonon interaction in such dots ($S \ll 1$), difficulties arise explaining the fact that the most intense satellite was not the one-LO-phonon sideband but rather the two-LO phonon or three-LO one. This effect was qualitatively understood as arising from a resonant coupling of the corresponding phonon replica of the ground state to the excited state of the exciton.[26] Considering a QD ensemble, one can think in terms of a multiphonon "filtering" of inhomogeneously distributed excited states.[27] However, when single QD spectroscopy is used,[26] such a resonance of the interlevel spacing with a multiple of the phonon energy is rather improbable. (Even though there are several confined optical phonon modes with slightly different energies, capable of considerable coupling to the exciton, this dispersion is only of the order of 1 meV.) The assumption of a reasonably strong off-diagonal coupling of the lowest and higher exciton states (not in a close resonance with a certain number of phonons) can account for anomalously strong n-LO-phonon sidebands. Figure 9 shows how peaks separated by energies approximately equal to that of the optical phonon can appear in the absorption spectra. We took a value of $\Delta = 55$ meV, typical of InAs/GaAs self-assembled QD's, and considered two optical phonon modes with the energies of 32 and 30 meV in order to simulate the experimental result of Lemaître *et al.*[26] (The two modes can be interpreted as a LO phonon in pure InAs and an InAs-like LO phonon in the $In_xGa_{1-x}As$ alloy near the QD boundary, respectively.) The values of $\alpha_{12}^\nu = 0.2$ and 0.15 used in this calculation do not look extraordinarily high taking into account the argument presented above [see Eq. (26)] and the possible contribution of the optical deformation potential mechanism in this interaction. A similar value ($\alpha_{12} = 0.15$) was used in Ref. 31 to explain the experimentally observed anticrossing of interlevel electron transitions with LO phonons in InAs QD's. We chose $p_{02} = p_{01}$ in the calculation since the upper level is also optically active in this case (notice that the relative value of p_{02} does not affect the positions of spectral features, just their intensities). As can be seen from Fig. 9, the second strong absorption peak is *not* separated from the ZPL by the energy Δ and can be called "two-LO satellite," since the weaker one-LO and three-LO replicas also show up in the spectrum. The calculated spec-
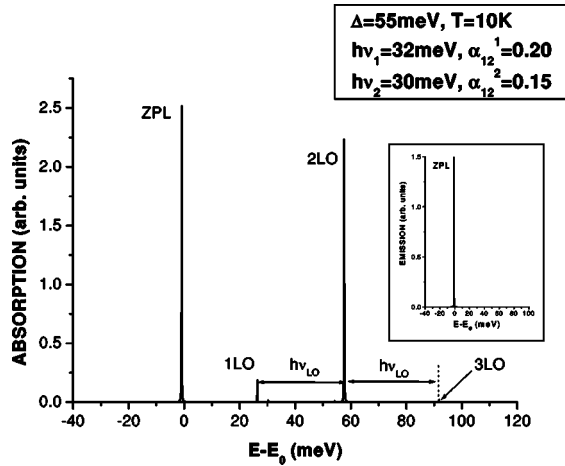
FIG. 9. Low-temperature absorption spectrum calculated for an InAs QD with the level spacing of $\Delta = 55$ meV assuming two optical phonon modes (the energies are given on the figure) and neglecting coupling to acoustic phonons. The interaction constants used in this calculation are $\alpha_{11}^1 = 0.005$, $\alpha_{22}^1 = 0.005$, $\alpha_{12}^1 = 0.2$; $\alpha_{11}^2 = 0.005$, $\alpha_{22}^2 = 0.005$, $\alpha_{12}^2 = 0.15$. Notice that three features above the zero-phonon line are separated by nearly the same energy, approximately equal to 31 meV. The inset shows the corresponding emission spectrum.

trum is in good agreement with the experimental observation of Ref. 26.

C. Homogeneous broadening of absorption lines

In structures of higher dimensionality the temperature dependence of the homogeneous linewidth is described by the following relation:

$$\Gamma(T) - \Gamma(0) = \gamma_{ac} n_{ac}(T) + \gamma_{LO} n_{LO}(T), \qquad (27)$$

where γ_{ac} and γ_{LO} are constants and n_{ac} and n_{LO} the Bose factors for the acoustic and optical phonons, respectively. There is no reason for Eq. (27) to be a good approximation for QD's, because it relies on the existence of a continuum of electronic states and also is limited to one-phonon scattering processes. Still it has been used in Refs. 15 and 19 and some other publications to qualitatively describe the dependence $\Gamma(T)$ extracted from experimental absorption spectra of spherical QD's. It was found that this dependence, in the region from 77 to 300 K, is much stronger than linear, similar to that predicted by the second term in Eq. (27), suggesting that there is some broadening related to the optical phonons. As has been pointed out in the Introduction, the interaction of localized electrons with optical phonons only produces additional discrete spectral lines. Consequently, the optical-phonon-related part of the broadening should not be taken literally; strictly speaking, the broadening occurs only because of the continuum of acoustic phonons. Our calculations in Fig. 8, where the interaction constants were taken as those for a typical spherical CdSe QD studied in Ref. 29, demonstrates this effect. The interaction with several optical phonon modes results in a series of closely spaced discrete peaks [see inset in Fig. 8] that is camouflaged by the acoustic

phonons. The effective homogeneous broadening of the spectral lines may apparently depend on the equilibrium number of acoustic and optical phonons. Nevertheless, Eq. (27) is too simple to describe this effect even qualitatively, as found in Ref. 51 using single QD spectroscopy.

Owing to the apparent similarity with systems of higher dimensionality, some authors associate the broadening discussed above with the optical-phonon-assisted carrier relaxation. However, it has been pointed out[33,38] that this is not a lifetime (or irreversible scattering) effect. Indeed, the polaron states considered here are stationary states. The phonon-assisted relaxation can probably occur through an anharmonic decay of the phonons participating in the formation of the polaronic states, as suggested in Refs. 38 and 52 and calculated in Ref. 36 and 53. Our consideration of the polaron spectrum in the presence of acoustic phonons shows, however, another possibility, namely, the acoustic-phonon-mediated transitions between different polaron states owing to the nondiagonal term in Eq. (24). The next step should consist of analyzing the efficiency of this mechanism. It is worth noting at this point that, contrary to the opinion of the authors of Ref. 37, such acoustic-phonon-mediated transitions in the polaron spectrum should not be subject to phonon bottleneck, because there are plenty of polaron states due to different optical phonon modes coupled differently to the exciton. Many of them (which do not necessarily show up in the spectra corresponding to thermal equilibrium) are separated by small energies within the band of acoustic phonons efficiently interacting with the polaron.

D. Up-converted PL

The up-converted or anti-Stokes photoluminescence (ASPL) involves the emission of photons with energies higher than the excitation energy (E_{exc}). This effect was observed for colloidal II-VI QD's and discussed in several recent publications.[54–56] Additional information can be found in Ref. 57. The ASPL occurs when an ensemble of QD's is excited at the very edge of the absorption spectrum, below the normal (i.e., excited with high-energy photons) PL band. The principal experimental facts concerning this effect are the following:

(i) The ASPL intensity increases linearly with the excitation power,[55] which can be rather low.

(ii) The blue (anti-Stokes) shift between the ASPL peak and E_{exc} does not significantly depend upon the QD size, if E_{exc} is chosen proportionally to the absorption peak energy (which depends upon the size).[55] However, the shift increases with temperature and can range from 20 to 150 meV.[57]

(iii) If E_{exc} increases (approaching the absorption peak) the ASPL also moves continuously towards higher energies.[55] Its intensity increases, and finally the spectrum transforms into the normal PL band.[57]

(iv) The ASPL intensity increases strongly with temperature.

Possible ASPL mechanisms were discussed in Refs. 54–56, but no definite conclusion was made. According to (i), processes like two-photon absorption and (since the pos-
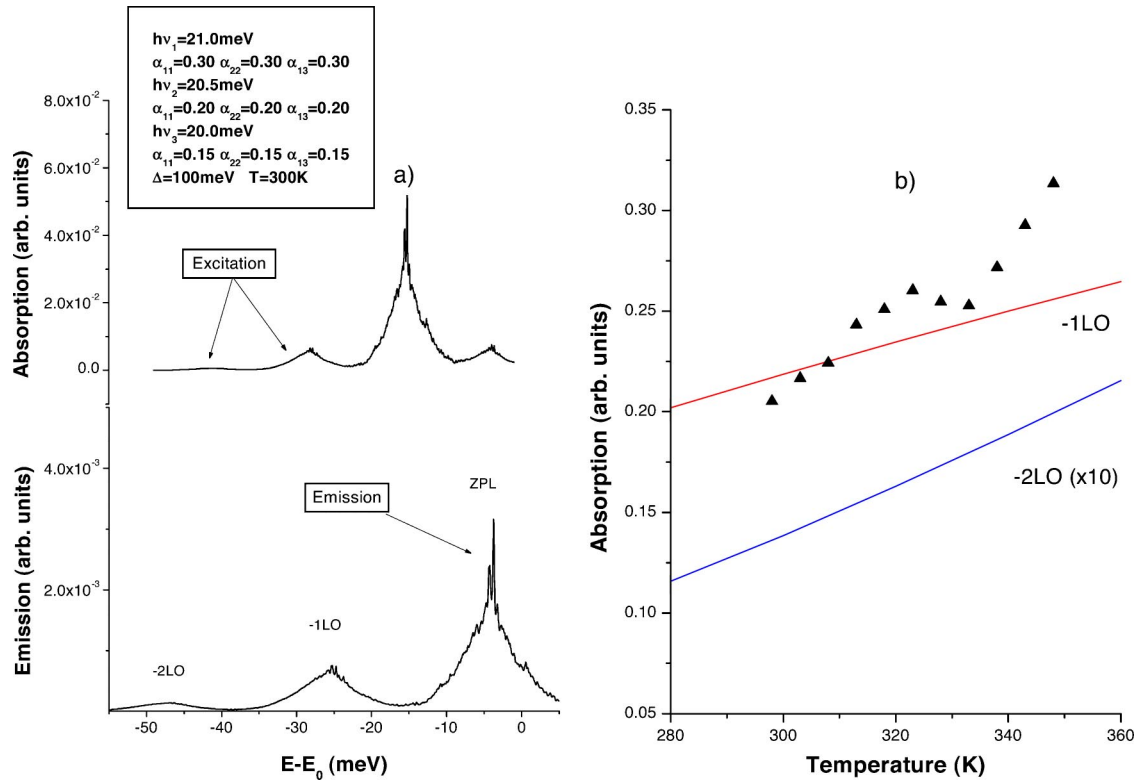
FIG. 10. (a) Low-energy part of the absorption and emission spectra calculated for a hypothetical CdTe QD considering three optical phonon modes with parameters given on the figure. The acoustic phonon parameters were taken as for Fig. 6. The level spacing $\Delta = 100$ meV, temperature 300 K. (b) Temperature dependence of the integrated intensity of two subgap bands in the absorption spectrum (a) (lines) and experimental data of Ref. 55 (points) showing the temperature dependence of the ASPL peak amplitude.

sibility of emergence of more than one exciton per QD is negligible) Auger excitation can be excluded in this case. Therefore, it was suggested that incident photons excite electrons to some intermediate subgap states from which they eventually proceed to the higher energy (luminescent) states through a thermal effect. Some obscure surface states (SS's) for which, as admitted by the authors of Ref. 56, there is not any direct evidence, were suggested as being responsible for the subgap absorption.[55,56]

From our point of view, the participation of subgap SS's (even if they exist in the passivated colloidal QD's) is unlikely in virtue of the experimental results (ii) and (iii). In fact, it would require the SS's energy to have approximately the same dependence on the QD size as that of the confined electronic states in the dots, in obvious contradiction with what should be expected from the general point of view. At the same time, naturally formed subgap states exist, which are separated from the fundamental absorption line (i.e., ZPL) by energies which are only weakly dependent on the QD size. These are the redshifted optical phonon replicas. In order to demonstrate this, we calculated polaron spectra of a spherical QD taking into consideration the $1s_e1S_{3/2}$ and $1s_e2S_{3/2}$ bare exciton states separated by some 100 meV, interacting with three strongest confined phonon modes with angular momenta $l=0,2$ (the coupling constants were taken approximately two times larger than the calculated values[39] in order to take into account other phonon modes not included explicitly). Figure 10(a) presents the lower-energy

side of a calculated QD absorption spectrum showing two subgap bands (designated as "-1LO" and "-2LO") through which the dot can be excited. The excited QD then will emit a photon, most likely having the ZPL energy. The probability of such an up-conversion process increases with temperature because the integrated intensity of "-1LO" and "-2LO" absorption bands [shown calculated in Fig. 10(b)] also increases. The experimental temperature dependence of the ASPL intensity measured in Ref. 55 can be understood taking into account that, at a certain temperature, further redshifted satellites (whose intensity depends more strongly on the temperature) become more efficient. The situation is complicated by the distribution of the QD size, so that E_{exc} can match different "-nLO" bands of dots of several different sizes. This agrees qualitatively with the experimentally observed increase in the anti-Stokes shift with temperature.[57] Modeling of the ensemble effects involved in the ASPL phenomenon is beyond the scope of this paper and will be considered in a future work. Nevertheless, we believe that our model explains, at least qualitatively, the principal experimental facts concerning ASPL.

In conclusion, we have proposed a nonperturbative approach for the calculation of the polaronic effects in QD's, which allows for the consideration of electronic levels coupled through the interaction with several confined phonon modes. Using this approach, we were able to show that the polaronic effects are significant, even when the interlevel spacing is quite far away from resonance with the optical

phonon energies. We have demonstrated that this opens the possibility to account for some previously published and not clearly understood phenomena in experimental data. We have also presented an explicit calculation of the spectral line shapes because of the diagonal interaction of acoustic phonons with the original electronic levels and suggest that the same interaction may be responsible for relaxation of the polaron entity to lower energies.

APPENDIX: ELECTRON–ACOUSTIC-PHONON COUPLING RATES

The following simple model was used to estimate the rates $\alpha_{\mathbf{q}}$ of electron coupling to longitudinal acoustic phonons. Assuming that LA phonons are completely delocalized, that is, neglecting acoustic impedance at the interface between the QD and matrix, the displacement can be written as

$$u_z = \left(\frac{\hbar}{2\omega_q \rho_0 V}\right)^{1/2} \mathrm{Re}\, e^{i(qz-\omega_q t)},$$

where ρ_0 is the density. For the deformation potential interaction mechanism the dimensionless coupling constant is[49]

$$\alpha_{\mathbf{q}} = \frac{a_c}{\hbar \omega_{\mathbf{q}}} \int |\psi|^2 \mathrm{div}\, \mathbf{u}(\mathbf{q}) dV,$$

where a_c is the bulk deformation potential and ψ the electron wave function. Considering the lowest conduction band state in a spherical QD of radius R, with infinite barriers, the wave function is[48]

$$\psi = \sqrt{\frac{1}{2\pi R}} \frac{\sin(\pi r/R)}{R}\; (r \leqslant R).$$

Using these expressions, we obtain

$$\alpha_{\mathbf{q}} = a_c \left(\frac{1}{2\hbar \omega_q \rho_0 V c_l^2}\right)^{1/2} I(qR), \qquad (A1)$$

where c_l is the longitudinal sound velocity,

$$I(y) = 2\pi^2 \int_0^1 j_0(yx) j_0^2(\pi x) x^2 dx, \qquad (A2)$$

and j_0 is the spherical Bessel function. The integral in (A2) can be expressed in terms of the integral sinus as

$$\frac{1}{2}\left\{\mathrm{Si}(y) - \frac{1}{2}[\mathrm{Si}(y+2\pi) + \mathrm{Si}(|y-2\pi|)]\right\}.$$

The function $I(y)$ decreases from 1 for $y=0$ to nearly zero for $y \geqslant 5$.

*Electronic address: mikhail@fisica.uminho.pt

†Electronic address: anda@fis.puc-rio.br

‡Electronic address: sergio@if.uff.br

[1] L. Bányai and S. W. Koch, *Semiconductor Quantum Dots* (World Scientific, Singapore, 1993).

[2] R. Heitz, in *Nano-Optoelectronics. Concepts, Physics, and Devices*, edited by M. Grundmann (Springer-Verlag, Berlin, 2002), p.239.

[3] T. D. Krauss, F. W. Wise, and D. B. Tanner, Phys. Rev. Lett. **76**, 1376 (1996).

[4] M. P. Chamberlain, C. Trallero-Giner, and M. Cardona, Phys. Rev. B **51**, 1680 (1995).

[5] M. I. Vasilevskiy, A. G. Rolo, M. V. Artemyev, S. A. Filonovich, M. J. M. Gomes, and Yu. P. Rakovich, Phys. Status Solidi B **224**, 599 (2001).

[6] M. I. Vasilevskiy, A. G. Rolo, M. J. M. Gomes, O. V. Vikhrova, and C. Ricolleau, J. Phys.: Condens. Matter **13**, 3491 (2001).

[7] E. P. Pokatilov, S. N. Klimin, V. M. Fomin, J. T. Devreese, and F. W. Wise, Phys. Rev. B **65**, 075316 (2002).

[8] P. Verma, W. Cordts, G. Irmer, and J. Monecke, Phys. Rev. B **60**, 5778 (1999).

[9] L. Savoit, B. Champagnon, E. Duval, I. A. Kudriavtsev, and A. I. Ekimov, J. Non-Cryst. Solids **197**, 238 (1996).

[10] D. A. Tenne, V. A. Haisler, A. I. Toropov, A. K. Bakarov, A. K. Gutakovsky, D. R. T. Zahn, and A. P. Shebanin, Phys. Rev. B **61**, 13 785 (2000).

[11] J. R. Huntzinger, J. Groenen, M. Cazayous, A. Mlayah, N. Bertru, C. Paranthoen, O. Dehaese, H. Carrére, E. Bedel, and G. Armelles, Phys. Rev. B **61**, R10 547 (2000).

[12] P. Palinginis, S. Tavenner, M. Lonergan, and H. Way, Phys. Rev. B **67**, 201307 (2003).

[13] T. Warming, F. Gufferth, R. Heitz, C. Kaptein, P. Brunkov, V. M. Ustinov, and D. Bimberg, Semicond. Sci. Technol. **19**, S51 (2004).

[14] B. Krummheuer, V. M. Axt, and T. Kuhn, Phys. Rev. B **65**, 195313 (2002).

[15] S. Nomura and T. Kobayashi, Phys. Rev. B **45**, 1305 (1992).

[16] Y. Cheng, S. Huang, J. Yu, and Y. Chen, J. Lumin. **60-61**, 786 (1994).

[17] R. Heitz, I. Mukhametzhanov, O. Stier, A. Madhukar, and D. Bimberg, Phys. Rev. Lett. **83**, 4654 (1999).

[18] M. G. Bawendi, P. J. Carroll, W. L. Wilson, and L. E. Brus, J. Chem. Phys. **96**, 946 (1992).

[19] V. Jungnickel and F. Henneberger, J. Lumin. **70**, 238 (1996).

[20] M. Bissiri, G. B. von Högersthal, A. S. Bhatti, M. Capizzi, A. Frova, P. Frigeri, and S. Franchi, Phys. Rev. B **62**, 4642 (2000).

[21] I. V. Ignatiev, I. E. Kozin, V. G. Davydov, S. V. Nair, J.-S. Lee, H.-W. Ren, S. Sugou, and Y. Masumoto, Phys. Rev. B **63**,

075316 (2001).

[22] V. M. Fomin, V. N. Gladilin, J. T. Devreese, E. P. Pokatilov, S. N. Balaban, and S. N. Klimin, Phys. Rev. B **57**, 2415 (1998).

[23] H. Rho, L. M. Robinson, L. M. Smith, H. E. Jackson, S. Lee, M. Dobrowolska, and J. K. Furdyna, Appl. Phys. Lett. **77**, 1813 (2000).

[24] S. Fafard, R. Leon, D. Leonard, J. L. Merz, and P. M. Petroff, Phys. Rev. B **52**, 5752 (1995).

[25] K. H. Schmidt, G. Medeiros-Ribeiro, M. Oestreich, P. M. Petroff, and G. H. Döhler, Phys. Rev. B **54**, 11 346 (1996).

[26] A. Lemaitre, A. D. Ashmore, J. J. Finley, D. J. Mowbray, M. S. Skolnick, M. Hopkinson, and T. F. Krauss, Phys. Rev. B **63**, 161309 (2001).

[27] Y. Toda, O. Moriwaki, M. Nishioka, and Y. Arakawa, Phys. Rev. Lett. **82**, 4114 (1999).

[28] R. Heitz, M. Veit, N. N. Ledentsov, A. Hoffmann, D. Bimberg, V. M. Ustinov, P. S. Kop'ev, and Zh. I. Alferov, Phys. Rev. B **56**, 10 435 (1997).

[29] Yu. P. Rakovich, M. I. Vasilevskiy, M. V. Artemiev, S. A. Filonovich, A. G. Rolo, D. J. Barber, and M. J. M. Gomes, in *Proceedings of the 25th International Conference on the Physics of Semiconductors*, edited by N. Miura and T. Ando (Springer, Berlin, 2001), Part II, p. 1203.

[30] S. Marcinkevicius, A. Gaarder, and R. Leon, Phys. Rev. B **64** 115307 (2001).

[31] S. Hameau, Y. Guldner, O. Verzelen, R. Ferreira, G. Bastard, J. Zeman, A. Lemaitre, and J. M. Gérard, Phys. Rev. Lett. **83**, 4152 (1999).

[32] J. T. Devreese, V. M. Fomin, V. N. Gladilin, E. P. Pokatilov, and S. N. Klimin, Nanotechnology **13**, 163 (2002); V. N. Gladilin, S. N. Balaban, V. M. Fomin, and J. T. Devreese, in *Proceedings of the 25th Conference on the Physics of Semiconductors*, edited by N. Miura and T. Ando (Springer, Berlin, 2001), Part II, p. 1243.

[33] T. Inoshita and H. Sakaki, Phys. Rev. B **56**, R4355 (1997).

[34] K. Král and Z. Khás, Phys. Rev. B **57**, R2061 (1998).

[35] T. Stauber, R. Zimmermann, and H. Castella, Phys. Rev. B **62**, 7336 (2000).

[36] O. Verzelen, R. Ferreira, and G. Bastard, Phys. Rev. Lett. **88**, 146803 (2002).

[37] L. Jasak, P. Machnikowski, J. Krasnyi, and R. Zöller, Eur. Phys. J. D **22**, 319 (2003).

[38] S. A. Levetas, M. J. Godfrey, and P. Dawson, in *Proceedings of 25th International Conference on the Physics of Semiconductors*, edited by N. Miura and T. Ando (Springer-Verlag, Berlin, 2001), part II, p. 1333.

[39] M. I. Vasilevskiy, E. V. Anda, and S. S. Makler, in *Proceedings of the 26th International Conference on the Physics of Semiconductors*, edited by A. R. Long and J. H. Davies, Institute of Physics Conference Series Number 171 (IOP, Bristol, 2002), P229.

[40] R. Zimmermann and R. Runge, in *Proceedings of the 26th International Conference on the Physics of Semiconductors*, edited by A. R. Long and J. H. Davies, Institute of Physics Conference Series Number 171 (IOP, Bristol, 2002), M3.1.

[41] S. Schmitt-Rink, D. A. B. Miller, and D. S. Chemla, Phys. Rev. B **35**, 8113 (1987).

[42] V. Savona, F. Bassani, and S. Rodriguez, Phys. Rev. B **49**, 2408 (1994).

[43] G. D. Mahan, *Many-Particle Physics* (Kluwer Academic, New York, 2000).

[44] P. Meystre and M. Surgent III, *Elements of Quantum Optics* (Springer-Verlag, Berlin, 1998), p. 287.

[45] J. Bonča and S. A. Trugman, Phys. Rev. Lett. **75**, 2566 (1995).

[46] S. S. Makler, E. V. Anda, R. G. Barrera, and H. M. Pastawski, Braz. J. Phys. **24**, 330 (1994).

[47] E. M. Lifshitz and L. P. Pitaevskii, *Statistical Physics, Part II* (Moscow, Nauka, 1978), p. 173.

[48] A. I. Ekimov, F. Hache, M. C. Schanne-Klein, D. Ricard, C. Flytzanis, I. A. Kudryavtsev, T. V. Yazeva, A. V. Rodina, and Al. L. Efros, J. Opt. Soc. Am. B **10**, 100 (1993).

[49] P. Y. Yu and M. Cardona, *Fundamentals of Semiconductors* (Springer-Verlag, Berlin, 1996).

[50] M. A. Odnoblyudov, I. N. Yassievich, and K. A. Chao, Phys. Rev. Lett. **83**, 4884 (1999).

[51] M. Bayer and A. Forchel, Phys. Rev. B **65**, 041308 (2002).

[52] X. Q. Li, H. Nakayama, and Y. Arakawa, Phys. Rev. B **59**, 5069 (1999).

[53] O. Verzelen, G. Bastard, and R. Ferreira, Phys. Rev. B **66**, 081308 (2002).

[54] E. Poles, D. C. Selmarten, O. I. Mićić, and A. J. Nozik, Appl. Phys. Lett. **75**, 971 (1999).

[55] Yu. P. Rakovich, S. A. Filonovich, M. J. M. Gomes, J. F. Donegan, D. V. Talapin, A. L. Rogach, and A. Eychmüller, Phys. Status Solidi B **229**, 449 (2002); Yu. P. Rakovich, A. A. Gladyshchuk, K. I. Rusakov, S. A. Filonovich, M. J. M. Gomes, D. V. Talapin, A. L. Rogach, and A. Eychmüller, Appl. Spectrosc. **69**, 444 (2002).

[56] X. Wang, W. W. Yu, J. Zhang, J. Aldana, X. Peng, and M. Xiao, Phys. Rev. B **68**, 125318 (2003).

[57] S. A. Filonovich, Ph.D. thesis, University of Minho, Braga, Portugal, 2003.